EARTHQUAKE ENGINEERING AND STRUCTURAL DYNAMICS
Earthquake Engng. Struct. Dyn. **27**, 1367–1383 (1998)

COVARIANCE CONTROL USING CLOSED-LOOP MODELLING FOR STRUCTURES

JIANBO LU[1,2] AND ROBERT R. SKELTON[3,*]

[1] *Structural Systems and Control Laboratory, Purdue University, U.S.A.*
[2] *Advanced Control Systems, Delphi Chassis Technical Center, General Motors, Dayton, OH, U.S.A.*
[3] *Department of Applied Mechanics & Engineering Sciences, University of California at San Diego, La Jolla, CA 92093-0411, U.S.A.*

SUMMARY

This paper presents a low-order controller design method, using closed-loop modelling plus covariance control, with application to the benchmark problem in structural control for the active mass drive system at the University of Notre Dame (see Reference 1). This method finds a satisfactory controller by iterating between the closed-loop modelling and the covariance control. The closed-loop modelling implies that the model used for model-based control design is extracted from the feedback system of the last iteration. The covariance control finds the optimal controller to minimize an output variance and at the same time to bound the other output variances. © 1998 John Wiley & Sons, Ltd.

KEY WORDS: modelling; identification; optimal control design; structural control

1. INTRODUCTION

Structural systems are typically dynamically rich. If we use the lumped parameter approximation finite-element method to model a structure, we might need hundreds or thousands of elements. This will generate a model of order of hundreds or thousands for the structure. If we use system identification and expect very accurate match between the identified model and the experimental data, then the identified model for the structure might also be of high order. The various modern control strategies usually provide a controller of the same order as the model. Hence, a high-order system model is not useful for an implementable, reliable and cost-effective control design. This raises a question about what models are suitable for control purposes. Here the philosophy is not the same as the open-loop response analysis where higher-order (finite element) models usually provide better results. The control objective dictates which system features must be preserved in the models. Hence the model used in control design must be a 'control oriented' one. A discussion about this can be found in References 2 and 3.

Besides the above control-modelling interaction issue, there is another interaction which also plays an important role in the closed-loop performance. This is the so-called *control-structure interaction*. Certain dynamics of the plant, do not exist in the open-loop environment, but appear in the closed-loop system. The neglected sensor and actuator dynamics can be cast into this category, since those dynamics are introduced into the closed-loop system with the control implementation. In Reference 4, this interaction is studied for protective structural systems and the results show that this interaction limits both the performance and the robustness.

* Correspondence to: Robert R. Skelton, Department of Applied Mechanics and Engineering Sciences, University of California at San Diego, La Jolla, CA 92093-0411, U.S.A. E-mail: bobskelton@ames.ucsd.edu

Contract/grant sponsor: NSF; Contract/grant number: CMS-9403592

CCC 0098–8847/98/111367–17$17·50

Received 1 August 1997
22 November 1997

Since both the control-modelling and the control-structure interactions can be reflected by the closed-loop system behaviour, a model which picks up the feedback information can serve as a control-oriented model. Therefore, a model generated from the closed-loop data will be a more appropriate one for control design. We call this *closed-loop modelling*. The closed-loop modelling indirectly handles those difficulties in structural control: limited control authority and modelling error. Another advantage of the closed-loop modelling is that the closed-loop system usually has larger damping than the open-loop system does. Hence, the amount of measured data to sufficiently capture the closed-loop system behaviour is smaller than the amount of data to capture an open-loop system behaviour.

The benchmark problem in structural control proposed by Spencer, Dyke and Deoskar[1] requires designing a compensator of limited complexity, based on a high-fidelity structure model, to achieve as stringent performance as possible. Hence, the control-modelling interaction in the benchmark problem could be very strong. The time delay, saturation, A/D and D/A effects in the closed-loop system also should be taken into account in order to find a high performance controller. Hence the combination of the closed-loop modelling with the control design is demanded for solving the benchmark problem.

In this paper, a low-order controller design method, using the closed-loop modelling through the so-called *q-Markov Cover*[5] plus the covariance control,[6] is studied, which is then applied for the active mass drive system. This method iterates between the closed-loop modelling and the covariance control. The covariance control finds an optimal controller to minimize an output variance and at the same time bounds the other output variances to specified values. The model identification technique used here is the so-called weighted noisy q-Markov Cover, which finds a state-space approximation of a physical system to match both the Markov and covariance parameters generated from the response data respect to white noise process inputs.

This paper is organized as follows. In Section 2, the control design problem for the active mass drive system is described. The closed-loop modelling using weighted noisy q-Markov Cover method is discussed in Section 3. Section 4 presents an iterative procedure to design a digital controller with prescribed output variance bounds. The iteration between the closed-loop modelling and the control design is considered in Section 5. The numerical work is described in Section 6. A brief conclusion is included in Section 7.

The following describe some notations used in this paper. A semi-positive-definite matrix X is denoted as $X \geqslant 0$. $\mathrm{tr}(\cdot)$ denote the trace for a matrix $(\cdot)$. $(\cdot)^+$ is the Moore–Penrose inverse of a matrix $(\cdot)$. $\mathbf{E}_\infty[\cdot]$ is the steady-state expectation operation. blockdiag$(\cdot)$ denotes a matrix whose block diagonal elements are matrices. z in $\mathbf{P}(z)$ is the variable used in z-transform for a digital transfer function.

2. CONTROL DESIGN PROBLEM OF THE ACTIVE MASS DRIVE SYSTEM

The active mass drive system at the University of Notre Dame described by Spencer, Dyke and Deoskar[1] can be depicted by the diagram shown in Figure 1. Where the output y_s with

$$y_s = [\, y_{s_1} \;\; y_{s_2} \;\; y_{s_3} \;\; y_{s_4} \;\; y_{s_5} \,]^T$$

represent the noisy sensor outputs used for measuring the following system signals:

$$[\, x_m \;\; \ddot{x}_1 \;\; \ddot{x}_2 \;\; \ddot{x}_3 \;\; \ddot{x}_m \,]^T$$

where x_m and $\ddot{x}_m$ are the displacement and the absolute acceleration of the active mass, $\ddot{x}_i$ is the absolute acceleration of the ith floor for $i = 1, 2, 3$. Notice that these signals are contaminated by the following additive noises in y_s:

$$w_s = [\, w_{s_1} \;\; w_{s_2} \;\; w_{s_3} \;\; w_{s_4} \;\; w_{s_5} \,]^T$$

i.e.

$$y_s = [\, x_m \;\; \ddot{x}_1 \;\; \ddot{x}_2 \;\; \ddot{x}_3 \;\; \ddot{x}_m \,]^T + w_s$$

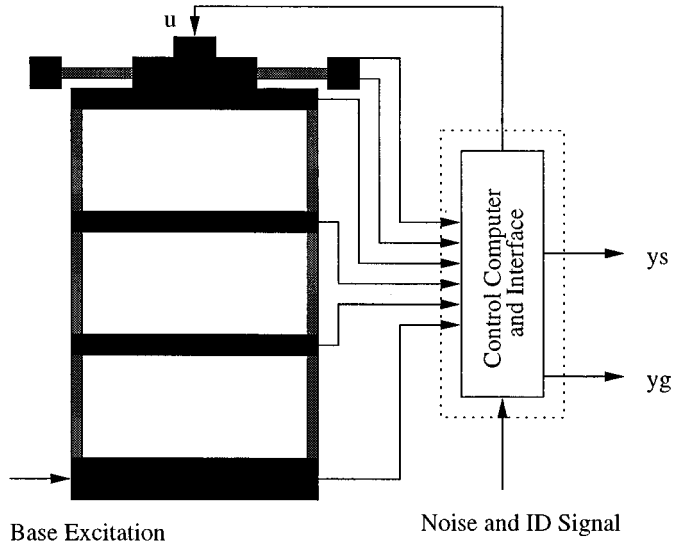

Figure 1. System setting of the controlled active mass drive system

y_g is the noisy sensor output for the ground acceleration $\ddot{x}_g$, i.e.

$$y_g = \ddot{x}_g + w_g$$

where w_g is the noise associated with the ground acceleration sensor.

Using block diagram, Figure 1 can be depicted in (a) of Figure 2 where P depicts the structure and includes the possible sensor and actuator dynamics. A high fidelity model of P, called the evaluation model, is determined from the data collected at SDC/EEL using the identification method presented in Dyke *et al.*[7] The state-space description of the evaluation model is

$$\begin{aligned} \dot{x} &= Ax + B(u + w_a) + E\ddot{x}_g \\ y_s &= C_y x + D_y(u + w_a) + F_y \ddot{x}_g \\ y_g &= \ddot{x}_g + w_g \\ z &= C_z x + D_z u + F_z \ddot{x} \end{aligned} \tag{1}$$

where w_a represents the noise associated with the actuator, K represents the control computer and the total sensor output is

$$y = [y_s^T \; y_g]^T.$$

For the implementation purpose, the algorithm used in the control computer must obey a digital law, i.e., we are interested in designing a digital control logic. In the following, the digital control logic for the control computer K is denoted as K. In this paper, this digital control logic K for which we are searching is a linear compensator with the following form:

$$\begin{aligned} x_{c_{k+1}} &= \mathsf{A}_c x_{c_k} + \mathsf{B}_c(y_k - D_y u_k) \\ u_k &= (I + \mathsf{D}_c D_y)^{-1}(\mathsf{C}_c x_{c_k} + \mathsf{D}_c y_k) \end{aligned} \tag{2}$$

where A_c, B_c, C_c, D_c are the controller parameters to be determined. Instead of designing a continuous time controller then discretizing the controller to obtain a digital one as in Spencer, Dyke and Deoskar,[1] we will

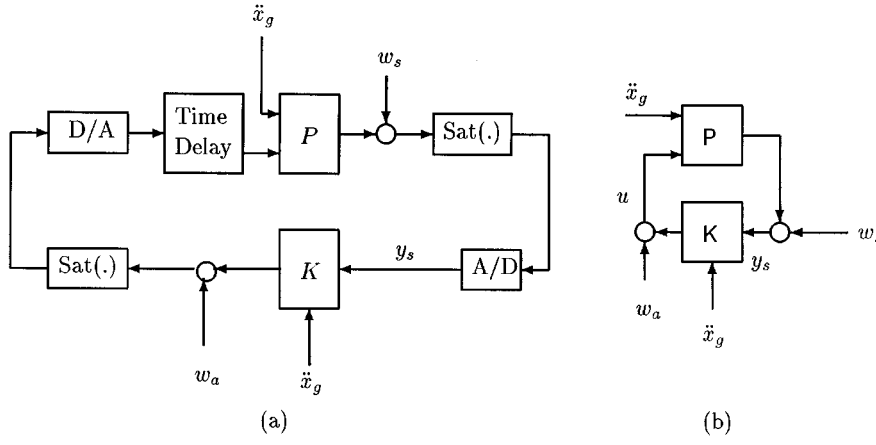

Figure 2. The block diagram description of the active mass drive system

design this digital controller directly from the discrete-time system P (see (b) of the Figure 2), where P is an augmented system including saturation non-linearities, time delay, A/D and D/A effects. A linear approximation $\hat{\mathsf{P}}$ of P is used to deduce a linear model.

Notice that since the sensor noise w_s is very small in the benchmark problem setting, and is not subject to the saturation, we can move the sensor noise w_s from the before-saturation location to the after-saturation location, as shown in (b) of Figure 2.

Hence for our approach, the benchmark problem can be specialized to the following.

Benchmark problem statement in active mass drive systems: Find a discrete time approximation (model) $\hat{\mathsf{P}}$ of the augmented plant P such that a digital control logic K of the form (2) can be found from $\hat{\mathsf{P}}$ which achieves the following

(i) The digital controller K is stable, of order $\leqslant 12$.
(ii) The sampling time of the digital controller K is $T_s = 0{\cdot}001$ s.
(iii) The closed-loop system by incorporating K in (b) of Figure 2 will have as small as possible performance indices $J_1 \sim J_{10}$, which are defined in Reference 1.
(iv) The closed-loop system by incorporating K in (b) of Figure 2 will satisfy (for the Kanai–Tajini spectrum ground excitation) the variance hard constraints

$$\mathbf{E}_\infty[u^2] \leqslant 1\ \mathrm{V}^2,\ \mathbf{E}_\infty[\ddot{x}_m^2] \leqslant 2\ \mathrm{g}^2,\ \mathbf{E}_\infty[x_m^2] \leqslant 3\,\mathrm{cm}^2 \tag{3}$$

and the peak value hard constraints

$$\max_k |u_k| \leqslant 3\ \mathrm{V},\ \max_k |\ddot{x}_{m_k}| \leqslant 6\ \mathrm{g},\ \max_k |x_{m_k}| \leqslant 9\ \mathrm{cm} \tag{4}$$

for 1940 El Centro and 1968 Hachinohe earthquake excitations.
(v) The magnitude of the loop gain must be below -5 db at all frequencies above 35 Hz.

Our approach here is an iterative one, which iterates between the modelling and control design and can be conceptually described as the following.

Closed-loop modelling: Identifying a discrete-time model $\hat{\mathsf{P}}$ for P at the sampling time $T_s = 0{\cdot}001$ with order $\leqslant 12$, based on the data generated from the closed-loop system in (b) of Figure 2 with respect to the white noise process inputs.

Full-order control design: Designing a full-order digital controller based on the discrete-time model $\hat{\mathsf{P}}$ obtained from the closed-loop modelling.

After a controller is designed, a simulation for the evaluation model in (a) of Figure 2 is performed. If (i), (iii)–(v) in the problem statement are satisfied, this controller could be a satisfactory one. If not, iterate between the closed-loop modelling and the control design. In the following sections, we will first discuss the closed-loop modelling, then the control design.

3. CLOSED-LOOP MODELLING

For a given controller K, a linear discrete-time model $\hat{\mathsf{P}}$ of the augmented plant P can be extracted from the identified closed-loop system. Consider the stable system depicted in (b) of Figure 2. First, we want to find a linear discrete-time model $\hat{\mathsf{T}}(\mathsf{P},\mathsf{K})$ for this closed-loop system. Then we will construct a linear discrete-time model $\hat{\mathsf{P}}$ for P based on $\hat{\mathsf{T}}(\mathsf{P},\mathsf{K})$. Where $\hat{\mathsf{T}}(\mathsf{P},\mathsf{K})$ denotes the transfer matrix

$$\text{from } [\ddot{x}_g \;\; v_a + w_a \;\; v_s^T + w_s^T \;\; v_g + w_g + \ddot{x}_g]^T \text{ to } y_s$$

as shown in Figure 3. v_a, v_s and v_g are white noise processes which are injected at the actuator and sensor locations in the closed-loop setting for the modelling or identification purpose. w_a, w_s and w_g are noises associated with the actuators and sensor, $\ddot{x}_g$ is the earthquake excitation. v_a, v_s, v_g, w_a, w_s, w_g and $\ddot{x}_g$ are uncorrelated white noise processes.

Let

$$y = [y_s^T \;\; y_g]^T$$

be the response of the closed-loop system in Figure 3 with respect to the inputs v_a, v_s, v_g, w_a, w_s, w_g and $\ddot{x}_g$. Define the following augmented variables:

$$v = \begin{bmatrix} \ddot{x} \\ v_a \\ v_y \end{bmatrix},\; w = \begin{bmatrix} 0 \\ w_a \\ w_y \end{bmatrix},\; v_y = \begin{bmatrix} v_s \\ \ddot{x}_g + v_g \end{bmatrix},\; w_y = \begin{bmatrix} w_s \\ w_g \end{bmatrix}$$

From the input–output data pair $(v + w, y)$ and a given integer q, the first q autocorrelation parameters of y can be computed from

$$R_{yy_i} = \lim_{N\to\infty} \frac{1}{N} \sum_{k=0}^{N-1} y_{k+i} y_k^T$$

and the first q crosscorrelation parameters between y and v can be computed from

$$R_{yv_i} = \lim_{N\to\infty} \frac{1}{N} \sum_{k=0}^{N-1} y_{k+i} v_k^T$$

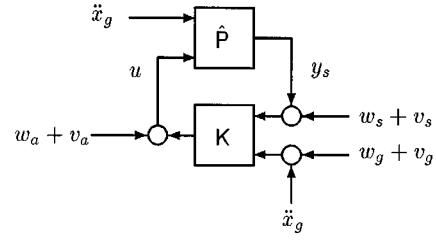

Figure 3. The block diagram for modelling purpose

the covariance of v can be computed from

$$V = \lim_{N\to\infty} \frac{1}{N} \sum_{k=0}^{N-1} v_k v_k^{\mathrm{T}}$$

which has the following structure:

$$V = \begin{bmatrix} X_{\mathrm{g}} & 0 & 0 & X_{\mathrm{g}} \\ 0 & V_{\mathrm{a}} & 0 & 0 \\ 0 & 0 & V_{\mathrm{s}} & 0 \\ X_{\mathrm{g}} & 0 & 0 & V_{\mathrm{g}} + X_{\mathrm{g}} \end{bmatrix}$$

with X_{g}, V_{a}, V_{s} and V_{g} being the variances or covariances of $\ddot{x}_{\mathrm{g}}$, v_{a}, v_{s} and v_{g}.

Assume that the associated noise w is a fixed covariance white noise with a known covariance W of the structure

$$W = \mathrm{blickdiag}(0, W_{\mathrm{a}}, W_{\mathrm{s}}, W_{\mathrm{g}})$$

where W_{a}, W_{s} and W_{g} are the variances or covariance of w_{a}, w_{s} and w_{g}.

Notice that in the practical computation, R_{yy_i}, R_{yv_i} and V are replaced by the following finite approximations:

$$R^N_{yy_i} = \frac{1}{N} \sum_{k=0}^{N-1} y_{k+i} y_k^{\mathrm{T}}$$

$$R^N_{yv_i} = \frac{1}{N} \sum_{k=0}^{N-1} y_{k+i} v_k^{\mathrm{T}}$$

$$V^N = \frac{1}{N} \sum_{k=0}^{N-1} v_k v_k^{\mathrm{T}}$$

for a sufficiently large integer N. In this paper, a typical value of N is 30 000.

The identification method used here finds a linear state-space model to match the following data set:

$$\mathrm{Data}_q \triangleq \{R_{yy_i}, R_{yv_i}, i = 0, 1, \ldots, q-1\}$$

A linear model (A_T, B_T, C_T, D_T) which matches the data set Data_q is called a *q-Markov Cover* (see Reference 5). The noisy q-Markov cover algorithm studied by Skelton and Shi,[8] and Skelton and Lu[9] finds such a linear model from the noisy measurement data pair $(v + w, y)$. In the following, we will give a brief discussion about this. Construct the following Toeplitz matrices:

$$\mathsf{R}_{yy_q} \triangleq \begin{bmatrix} R_{yy_0} & R^{\mathrm{T}}_{yy_1} & \cdots & R^{T}_{yy_{q-1}} \\ R_{yy_1} & R_{yy_0} & \cdots & R^{T}_{yy_{q-2}} \\ \vdots & \vdots & \ddots & \vdots \\ R_{yy_{q-1}} & R_{yy_{q-2}} & \cdots & R_{yy_0} \end{bmatrix}$$

$$\mathsf{R}_{yv_q} \triangleq \begin{bmatrix} R_{yv_0} & 0 & \cdots & 0 \\ R_{yv_1} & R_{yv_1} & \cdots & 0 \\ \vdots & \vdots & \ddots & \vdots \\ R_{yv_{q-1}} & R_{yv_{q-2}} & \cdots & R_{yv_0} \end{bmatrix}$$

and based on these two Toeplitz matrices compute

$$\mathsf{D}_q = \mathsf{R}_{yy_q} - \mathsf{R}_{yv_q}\mathsf{V}^{-1}(\mathsf{V}+\mathsf{W})\mathsf{V}^{-\mathrm{T}}\mathsf{R}_{yv_q}^{\mathrm{T}}$$

where

$$\mathsf{V} = \text{blockdiag}(V, V, \ldots, V)$$

$$\mathsf{W} = \text{blockdiag}(W, W, \ldots, W)$$

If $\mathsf{D}_q \geqslant 0$, find a full rank matrix factor O_q

$$\mathsf{D}_q = \mathsf{O}_q\mathsf{O}_q^{\mathrm{T}}$$

and compute

$$\mathsf{M}_q = [R_{yv_0}^{\mathrm{T}} \;\; R_{yv_1}^{\mathrm{T}} \;\; \cdots \;\; R_{yv_q}^{\mathrm{T}}]^{\mathrm{T}} V^{-1}$$

$$\mathsf{O}_{q-1} = [I_{n_y(q-1)} \;\; 0]\mathsf{O}_q$$

Then the state-space coefficient matrices (A_T, B_T, C_T, D_T) of the system in Figure 3 can be computed as

$$B_T = \tilde{B}_T(V+W)^{-1/2}$$

and

$$\begin{bmatrix} D_T & C_T \\ \tilde{B}_T & A_T \end{bmatrix} = \begin{bmatrix} I & 0 \\ 0 & \mathsf{O}_{q-1}^{+} \end{bmatrix} [\mathsf{M}_q \;\; \mathsf{O}_q].$$

Remark: The above system description is a particular q-Markov Cover. All the q-Markov covers can be found in References 5, 8 and 9, by adding a certain free unitary matrix.

Assume that the obtained linear model has the following transfer matrix:

$$\hat{\mathsf{T}}(\mathsf{P},\mathsf{K}) = D_T + C_T(zI - A_T)^{-1}B_T,$$

$$= [T_{\mathrm{ga}}(z) \;\; T_{\mathrm{s}_1}(z) \;\; T_{\mathrm{s}_2}(z)]$$

and the state-spaced descriptions of $T_{\mathrm{ga}}(z)$, $T_{\mathrm{s}_1}(z)$ and $T_{\mathrm{s}_2}(z)$ can be obtained from (A_T, B_T, C_T, D_T) as

$$T_{\mathrm{ga}}(z) = D_{\mathrm{ga}} + C_T(zI - A_T)^{-1}B_{\mathrm{ga}}$$

$$T_{\mathrm{s}_1}(z) = D_{\mathrm{s}_1} + C_T(zI - A_T)^{-1}B_{\mathrm{s}_1}$$

$$T_{\mathrm{s}_2}(z) = D_{\mathrm{s}_2} + C_T(zI - A_T)^{-1}B_{\mathrm{s}_2}$$

where

$$D_T = [D_{\mathrm{ga}} \;\; D_{\mathrm{s}_1} \;\; D_{\mathrm{s}_2}]$$

$$B_T = [B_{\mathrm{ga}} \;\; B_{\mathrm{s}_1} \;\; B_{\mathrm{s}_2}]$$

or from the following input–output relationship:

$$\begin{aligned} y_{\mathrm{s}} &= \hat{\mathsf{T}}(\mathsf{P},\mathsf{K})(v+w) \\ &= T_{\mathrm{ga}}(z)\begin{bmatrix} \ddot{x}_{\mathrm{g}} \\ v_{\mathrm{a}} + w_{\mathrm{a}} \end{bmatrix} + T_{\mathrm{s}_1}(z)(v_{\mathrm{s}} + w_{\mathrm{s}}) + T_{\mathrm{s}_2}(z)(v_{\mathrm{g}} + w_{\mathrm{g}} + \ddot{x}_{\mathrm{g}}) \end{aligned} \tag{5}$$

Now, we want to extract a linear model for P from equation (5), where the state-space descriptions of all the transfer matrices are already identified. From Figure 3, we have

$$y = \begin{bmatrix} y_s \\ y_g \end{bmatrix} = w_y + v_y + \begin{bmatrix} \hat{\mathsf{P}}(z) \\ 0 \end{bmatrix} \begin{bmatrix} \ddot{x}_g \\ u \end{bmatrix}$$

$$u = v_a + w_a + \mathsf{K}(z)y$$

This implies

$$y = \left(I - \begin{bmatrix} \hat{\mathsf{P}}(z) \\ 0 \end{bmatrix} \begin{bmatrix} 0 \\ \mathsf{K}(z) \end{bmatrix} \right)^{-1} \begin{bmatrix} \hat{\mathsf{P}}(z) & I & 0 \\ 0 & 0 & I \end{bmatrix} \begin{bmatrix} \ddot{x}_g \\ v_a + w_a \\ v_y + w_y \end{bmatrix} \tag{6}$$

Denote

$$\left(I - \begin{bmatrix} \hat{\mathsf{P}}(z) \\ 0 \end{bmatrix} \begin{bmatrix} 0 \\ \mathsf{K}(z) \end{bmatrix} \right)^{-1} = \begin{bmatrix} T_{11}(z) & T_{12}(z) \\ T_{21}(z) & T_{22}(z) \end{bmatrix}$$

with a partitioned dimensions compatible to the dimensions of y_s and y_g. It is obvious that $T_{11}(z)$ is invertible. Equation (6) can now be written as

$$\begin{bmatrix} y_s \\ y_g \end{bmatrix} = \begin{bmatrix} T_{11}(z)\hat{\mathsf{P}}(z) \\ T_{21}(z)\hat{\mathsf{P}}(z) \end{bmatrix} \begin{bmatrix} \ddot{x}_g \\ v_a + w_a \end{bmatrix} + \begin{bmatrix} T_{11}(z) \\ T_{21}(z) \end{bmatrix} (v_s + w_s) + \begin{bmatrix} T_{12}(z) \\ T_{22}(z) \end{bmatrix} (v_g + w_g + \ddot{x}_g) \tag{7}$$

Comparing Equations (5) with (7), $T_{11}(z)$ and $\hat{\mathsf{P}}(z)$ can be expressed from the identified transfer function $T_{ga}(z)$ and $T_{s_1}(z)$

$$T_{11}(z)\hat{\mathsf{P}}(z) = T_{ga}(z)$$

$$T_{11}(z) = T_{s_1}(z)$$

Hence, the transfer matrix of $\hat{\mathsf{P}}$ can be computed from

$$\hat{\mathsf{P}}(z) = T_{s_1}^{-1}(z)\, T_{ga}(z) \tag{8}$$

and the state-space description for equation (8) can be further obtained as

$$\hat{\mathsf{P}}(z) = D_P + C_P(zI - A_P)^{-1} B_P$$

where the state-space system matrices are

$$A_P = A_T - B_{s_1} D_{s_1}^{-1} C_T$$

$$B_P = B_{ga} - B_{s_1} D_{s_1}^{-1} D_{ga}$$

$$C_P = D_{s_1}^{-1} C_T$$

$$D_P = D_{s_1}^{-1} D_{ga}$$

Notice that $T_{11}(z)$ is invertible implies $T_{s1}(z)$ is invertible, so is D_{s_1}. The state-space model (A_P, B_P, C_P, D_P) is of the same order as the closed-loop system (A_T, B_T, C_T, D_T) and this plant model generated from the closed-loop system has been used in Skelton and Lu.[3,9]

4. COMPENSATOR DESIGN

Consider the discrete-time model $\hat{\mathsf{P}}$ obtained from the closed-loop modelling in the last section

$$\begin{aligned} x_{k+1} &= \hat{A}x_k + \hat{B}u_k + \hat{E}\ddot{x}_{g_k} \\ z_k &= \hat{C}_z x_k + \hat{D}_z u_k + \hat{F}_z \ddot{x}_{g_k} \\ y_k &= \hat{C}_y x_k + \hat{D}_y u_k + \hat{F}_y \ddot{x}_{g_k} + w_k \end{aligned} \tag{9}$$

where x represents the system state, z denotes the performance variable, u is the control variable, y is the measurement. Notice that the case where the direct measurement of the disturbance $\ddot{x}$ can also be cast into the above form: let $y = [y_s^T \; y_g]^T$, then

$$y = \begin{bmatrix} y_s \\ y_g \end{bmatrix} = \begin{bmatrix} \hat{C}_y \\ 0 \end{bmatrix} x_k + \begin{bmatrix} \hat{D}_y \\ 0 \end{bmatrix} u_k + \begin{bmatrix} \hat{F}_y \\ I \end{bmatrix} \ddot{x}_g + \begin{bmatrix} w_s \\ w_g \end{bmatrix}$$

Hence in the following, we will work on the general plant (9) instead of the discrete-time version of equation (1). We assume $(\hat{A}, \hat{C}_y)$ is detectable and $(\hat{A}, \hat{B})$ is stabilizable.

Denote $\mathscr{K}$ as the set of all controllers which (i) stabilize the evaluation model of the system; (ii) satisfy the loop gain constraint; (iii) make the closed-loop variables meet the hard constraints in equations (3) and (4). The benchmark problem require evaluation of

$$J_i, \; i = 1, 2, \ldots, 10 \tag{10}$$

The multiple performance criteria (J_i's) involve some specific disturbance sources (historical earthquake records and disturbances with the Kanai–Tajimi spectrums) and hard constraints. There are no systematic methods to exactly solve the above problem. Instead, we model the earthquake disturbances as white noise processes and solve the following problem:

$$\min_{\mathsf{K} \in \mathscr{K}} \mathbf{E}_\infty [z_j^2] \tag{11}$$

where z_j's reflect the variables involved in computing the performance indices J_i's. In this paper, due to the closed-loop modelling feature, we only take those measured variables as the performance variables, i.e., we have

$$z = [x_m \;\; \ddot{x}_1 \;\; \ddot{x}_2 \;\; \ddot{x}_3 \;\; \ddot{x}_m \;\; u]^T$$

A solvable control problem which indirectly reflects the objectives in equation (10) or (11) can be further expressed in the following constrained optimization problem:

$$\min_{\mathsf{K}} \{\mathbf{E}_\infty [z_0^T R z_0], \mathbf{E}_\infty [z_1^2] \leqslant \bar{Z}_1, \mathbf{E}_\infty [z_2^2] \leqslant \bar{Z}_2, \ldots, \mathbf{E}_\infty [z_n^2] \leqslant \bar{Z}_n\} \tag{12}$$

where n is the dimension of z, z_0 is a vector variable of the following form:

$$z_{0_k} = \hat{C}_0 x_k + \hat{D}_0 u_k + \hat{F}_0 \ddot{x}_{g_k}$$

equation (12) is similar to the so-called Output Variance Control (OVC) problem in Skelton.[6] It has been shown that a deterministic interpretation of the variance constraint is the peak value constraint.

The above consideration leads to our approach for the benchmark problem, which can be summarized as the follows: solving the optimization, problem (10) indirectly (i) by tuning $\bar{Z}_1, \bar{Z}_2, \ldots, \bar{Z}_n$ and solving the optimization problem in equation (12) which takes care of the stabilization and hard constraints; (ii) by incorporating the closed-loop modelling with equation (12) which takes care of the control order limitation; (iii) by simulation through the high fidelity evaluation model which finally validates the controller.

Now let us solve the optimization problem (12). Consider the following observer-based controller:

$$x_{c_{k+1}} = \hat{A}x_{c_k} + \hat{B}u_k + B_c(y_k - \hat{D}_y u_k - \hat{C}_y x_{c_k})$$
$$u_k = C_c x_{c_k} + D_c(y_k - \hat{D}_y u_k - \hat{C}_y x_{c_k}) \tag{13}$$

Using equation (13) to stabilize equation (9) leads to the following closed-loop system:

$$\tilde{x}_{k+1} = (\hat{A} - B_c\hat{C}_y)\tilde{x}_k + (\hat{E} - B_c\hat{F})\ddot{x}_{g_k} - B_c w_k \tag{14}$$

$$x_{c_{k+1}} = (\hat{A} + \hat{B}C_c)x_{c_k} + (\hat{B}D_c + B_c)(\hat{C}_y\tilde{x}_k + \hat{F}\ddot{x}_{g_k} + w_k) \tag{15}$$

$$z_k = (\hat{C}_z + \hat{D}_z C_c)x_{c_k} + \hat{C}_z\tilde{x}_k + \hat{D}_z D_c(\hat{C}_y\tilde{x}_k + \hat{F}_z\ddot{x}_{g_k} + w_k) + \hat{F}_z\ddot{x}_{g_k} \tag{16}$$

where $\tilde{x}_k = x_k - x_{c_k}$ is the state estimate error.

If we assume $\ddot{x}_{g_k}$ and w_k as white noise processes with covariances X_g and W, then using equation (14) the covariance of the state estimate error $\tilde{x}$ satisfies

$$\tilde{X} = (\hat{A} - B_c\hat{C}_y)\tilde{X}(\hat{A} - B_c\hat{C}_y)^T + (\hat{E} - B_c\hat{F})X_g(\hat{E} - B_c\hat{F})^T + B_c W B_c^T \tag{17}$$

for any B_c such that $\hat{A} - B_c\hat{C}_y$ is asymptotically stable. Notice that the existence of such B_c is guaranteed by the fact that $(\hat{A}, \hat{C}_y)$ is a detectable pair.

One can prove that the separation principle between the state feedback and the state estimator holds by following the same procedure as in Reference 6. Hence from equation (15) the covariance of the control state x_c satisfies

$$X_c = (\hat{A} + \hat{B}C_c)X_c(\hat{A} + \hat{B}C_c)^T + (\hat{B}D_c + B_c)\Psi(\hat{B}D_c + B_c)^T \tag{18}$$

for any C_c such that $\hat{A} + \hat{B}C_c$ is asymptotically stable. Notice that the existence of such C_c is guaranteed by the fact that $(\hat{A}, \hat{B})$ is a stabilizable pair. Where

$$\Psi = \hat{C}_y\tilde{X}\hat{C}_y^T + \hat{F}X_g\hat{F}^T + W \tag{19}$$

Consider that a digital controller K solving the optimization problem (12) is equivalent to that K solving the following problem for some q_i, $i = 1, 2, \ldots, n$ (see References 6 and 10):

$$\min_{\mathsf{K}} \{\mathbf{E}_\infty[z_0^T R z_0] + \mathbf{E}_\infty[z^T Q z]\} \tag{20}$$

where $Q = \mathrm{diag}(q_1, q_2, \ldots, q_n)$ and $z = [z_1 \;\; z_2 \;\; \cdots \;\; z_n]^T$. Denote

$$\hat{z} = \begin{bmatrix} \sqrt{R} & 0 \\ 0 & \sqrt{Q} \end{bmatrix} \begin{bmatrix} z_0 \\ z \end{bmatrix}$$

the cost function in (20) is $\mathbf{E}_\infty[\hat{z}^T\hat{z}]$ where

$$\hat{z} = Cx_k + D_u u_k + D_g\ddot{x}_{g_k}$$

and

$$C = \begin{bmatrix} \sqrt{R}\hat{C}_0 \\ \sqrt{Q}\hat{C}_z \end{bmatrix}, \quad D_u = \begin{bmatrix} \sqrt{R}\hat{D}_0 \\ \sqrt{Q}\hat{D}_z \end{bmatrix}, \quad D_g = \begin{bmatrix} \sqrt{R}\hat{F}_0 \\ \sqrt{Q}\hat{F}_z \end{bmatrix} \tag{21}$$

Hence from equation (16) and considering the separation principle, the variance of $\hat{z}$ can be computed as the following:

$$\mathbf{E}_\infty[\hat{z}^T\hat{z}] = \mathrm{tr}\{(C + D_u C_c)X_c(C + D_u C_c)^T + C\tilde{X}C^T + \; + D_u D_c\Psi D_c^T D_u^T + D_g X_g D_g^T\} \tag{22}$$

Notice that from equation (18), X_c can be written as

$$X_c = \sum_{k=0}^{\infty} (\hat{A} + \hat{B}C_c)^k (\hat{B}D_c + B_c)\Psi(\hat{B}D_c + B_c)^T (\hat{A} + \hat{B}C_c)^{Tk}$$

By substituting this X_c into equation (22) and using the property of the $\mathrm{tr}(\cdot)$ operation

$$\mathrm{tr}(NM) = \mathrm{tr}(MN)$$

equation (22) can be expressed as

$$\mathbf{E}_\infty[\hat{z}^T\hat{z}] = \mathrm{tr}\left\{\Psi(\hat{B}D_c + B_c)^T \left[\sum_{k=0}^{n} (\hat{A} + \hat{B}C_c)^k (C + D_u C_c)(C + D_u C_c)^T (\hat{A} + \hat{B}C_c)^{Tk}\right](\hat{B}D_c + B_c)\right\}$$
$$+ \mathrm{tr}(C\tilde{X}C^T + D_u D_c \Psi D_c^T D_u^T + D_g X_g D_g^T)$$

If we denote

$$Y_c = \sum_{k=0}^{n} (\hat{A} + \hat{B}C_c)(C + D_u C_c)(C + D_u C_c)^T (\hat{A} + \hat{B}C_c)^{Tk}$$

then Y_c satisfies the following Lyapunov equation:

$$Y_c = (\hat{A} + \hat{B}C_c)^T Y_c (\hat{A} + \hat{B}C_c) + (C + D_u C_c)^T (C + D_u C_c) \tag{23}$$

and equation (22) can be replaced by the following:

$$\mathbf{E}_\infty[\hat{z}^T\hat{z}] = \mathrm{tr}\{\Psi[(\hat{B}D_c + B_c)^T Y_c (\hat{B}D_c + B_c) + D_c^T D_u^T D_u D_c]\} + \mathrm{tr}\{C\tilde{X}C^T + D_g X_g D_g^T\} \tag{24}$$

Therefore, the optimization problem of equation (20) can be equivalently: expressed as the following constrained optimization:

$$J_{\mathrm{opt}} = \min_{D_c, C_c, Y_c, B_c, \tilde{X}} \{\mathbf{E}_\infty[\hat{z}^T\hat{z}], \quad \text{equations (17), (23), (24)}\}$$
$$= \min_{D_c} \min_{C_c, Y_c} \min_{B_c, \tilde{X}} [\mathbf{E}_\infty[\hat{z}^T\hat{z}], \quad \text{equations (17), (23), (24)}\} \tag{25}$$

From equation (24), we have

$$\frac{\partial \mathbf{E}_\infty[\hat{z}^T\hat{z}]}{\partial \tilde{X}} = C^T C + \hat{C}_y^T D_c^T D_u^T D_c \hat{C}_y \geqslant 0$$

hence in order to minimize $\mathbf{E}_\infty[\hat{z}^T\hat{z}]$, we must minimize $\tilde{X}$ which depends on B_c (see equation (17)). By using the completion of squares, the optimal B_c which minimizes $\tilde{X}$ can be computed as (see Reference 6)

$$B_c = (\hat{A}X\hat{C}_y^T + \hat{E}X_g\hat{F}_y)(\hat{C}_y X \hat{C}_y^T + \hat{F}_y X_g \hat{F}_y^T)^{-1} \tag{26}$$

where the optimal state error covariance satisfies

$$\tilde{X} = \hat{A}\tilde{X}\hat{A}^T + \hat{E}X_g\hat{E}^T - (\hat{A}\tilde{X}\hat{C}_y^T + \hat{E}X_g\hat{F}_y^T)\Psi^{-1}(A\tilde{X}\hat{C}_y^T + \hat{E}X_g\hat{F}_y)^T \tag{27}$$

and Ψ is defined in equation (19). Hence, we have

$$J_{\mathrm{opt}} = \min_{D_c} \min_{C_c, Y_c} \{\mathbf{E}_\infty[\hat{z}^T\hat{z}], \quad \text{equations (27), (23) and (24)}\}$$

From equation (24), we have

$$\frac{\partial \mathbf{E}_\infty[\hat{z}^T\hat{z}]}{\partial Y_c} = (\hat{B}D_c + B_c)\Psi(\hat{B}D_c + B_c)^T \geqslant 0$$

This implies that in order to minimize $\mathbf{E}_\infty[\hat{z}^T\hat{z}]$, we must minimize Y_c which depends only on C_c (see equation (23)). The optimal C_c which minimizes Y_c can be computed as

$$C_c = -\Phi^{-1}(\hat{A}^T Y_c \hat{B} + C^T D_u)^T \tag{28}$$

where the smallest Y_c is the solution of the following Riccati equation

$$Y_c = A^T Y_c A + C^T C - (\hat{A}^T Y_c \hat{B} + C^T D_u)\Phi^{-1}(\hat{A}^T Y_c \hat{B} + C^T D_u)^T \tag{29}$$

and

$$\Phi = (\hat{B}^T Y_c \hat{B} + D_u^T D_u) \tag{30}$$

Hence, the optimal value of the cost function can be further simplified to

$$J_{\text{opt}} = \min_{D_c} \{\mathbf{E}_\infty[\hat{z}^T\hat{z}], \quad \text{equations (27), (29) and (24)}\}$$

and the optimal D_c can be found as

$$D_c = -\Phi^{-1}\hat{B}^T Y_c B_c$$

Combining the above consideration with the weight Q updating method, we obtain the following Generalized Output Variance Control (GOVC) algorithm. For a set of given variance bounds $\bar{Z}_1, \bar{Z}_2, \ldots, \bar{Z}_n$, this algorithm finds a controller (13) solving equation (12). The reason that we call the constrained optimization problem (12) the Generalized Output Variance Control problem is due to: (i) GOVC generalizes the so-called OVC problem studied by Zhu and Skelton[10] and Skelton,[6] where $z_0 = u$ and z is a linear combination of the plant states and does not include the control variable u; (ii) GOVC deals with generalized plant description of the form equation (9) and the controller found in the GOVC algorithm is not limited to be strictly proper. This algorithm can be summarized as the follows.

Generalized Output Variance Control Algorithm:

Step 1: Solve for $\tilde{X}$ from the Riccati equation (27) and compute the control parameter B_c from equation (26).

Step 2. Choose an initial $Q_0 = \text{diag}(q_{01}, q_{02}, \ldots, q_{0n}) > 0$ and compute Y_c from the following Riccati equation:

$$\begin{aligned} Y_c = {} & \hat{A}^T Y_c \hat{A} + \hat{C}_0^T R \hat{C}_0 + \hat{C}_z^T Q_0 \hat{C}_z \\ & - (\hat{A}^T Y_c \hat{B} + \hat{C}_0^T R \hat{D}_0 + \hat{C}_z^T Q_0 \hat{D}_z)\Phi^{-1}(\hat{A}^T Y_c \hat{B} + \hat{C}_0^T R \hat{D}_0 + \hat{C}_z^T Q_0 \hat{D}_z)^T \end{aligned}$$

where $\Phi = \hat{B}^T Y_c \hat{B} + \hat{D}_0^T R \hat{D}_0 + \hat{D}_z^T Q_0 \hat{D}_z$. Compute the control parameters

$$D_c = -\Phi^{-1}\hat{B}^T Y_c B_c$$

$$C_c = -\Phi^{-1}(\hat{A}^T Y_c \hat{B} + \hat{C}_0^T R \hat{D}_0 + \hat{C}_z^T Q_0 \hat{D}_z)^T$$

Step 3. Compute X_c by solving the following Lyapunov equation:

$$X_c = (\hat{A} + \hat{B}C_c)X_c(\hat{A} + \hat{B}C_c)^T + (\hat{B}D_c + B_c)(\hat{C}_y \tilde{X} \hat{C}_y^T + \hat{F}_y X_g \hat{F}_y^T + W)(\hat{B}D_c + B_c)^T$$

Step 4. Compute the output covariance of z

$$\begin{aligned} Z = {} & (\hat{C}_z + \hat{D}_z D_c \hat{C}_y)\tilde{X}(\hat{C}_z + \hat{D}_z D_c \hat{C}_y)^T + (\hat{C}_z + \hat{D}_z C_c) X_c (\hat{C}_z + \hat{D}_z C_c)^T \\ & (\hat{F}_z + \hat{D}_z D_c \hat{F}_y) X_g (\hat{F}_z + \hat{D}_z D_c \hat{F}_y)^T \end{aligned}$$

Let Z_{ii} be the ith diagonal element of Z. For a given integer β (which affects the convergence rate of the algorithm), compute

$$q_i = \left\{\frac{Z_{ii}}{\bar{Z}_i}\right\}^{\beta} q_{i0} \quad \text{If } \sum_{i=1}^{n} |q_i - q_{0i}| < \varepsilon$$

go to step 5. Otherwise, set $q_i \to q_{i0}$ and go to step 2, where ε is the error tolerance.

Step 5. The system matrices of the controller (2) can be formulated as

$$\begin{aligned} \mathsf{A}_c &= \hat{A} + \hat{B}C_c - B_c\hat{C}_y - \hat{B}D_c\hat{C}_y \\ \mathsf{B}_c &= B_c + \hat{B}D_c \\ \mathsf{C}_c &= C_c - D_c\hat{C}_y \\ \mathsf{D}_c &= D_c \end{aligned} \tag{31}$$

Remark. Notice that for a given Q_0 and R, the steps 1 and 2 generate an LQG controller of the form equation (31) for the cost function (20). This problem is also a special case of the so-called multiobjective H_2 control problem studied by using the Linear Matrix Inequality as in Boyd *et al.*[11] The above GOVC algorithm can be easily realized in Matlab by using the discrete-time algebraic Riccati equation solver.

5. INTEGRATION OF CLOSED-LOOP MODELLING AND CONTROL

The following is the procedure we used to find a satisfactory controller for the benchmark control problem.

Step 1: Let $\bar{Z}_i$ for $i = 1, 2, \ldots, n$ be the output variance bounds. Choose integer q (number of Markov/covariance parameters to be matched) and integer N (length of the experimental data). Set $i = 0$ and $\hat{\mathsf{P}}_0$ as the evaluation model.

Step 2: *GOVC controller design*: Do model reduction using q-Markov cover for $\hat{\mathsf{P}}_i$ to obtain a lower-order model $\hat{\mathsf{P}}_{ir}$. Choose variance performance bounds κ_j, $j = 1, 2, \ldots, n$, for the design model $\hat{\mathsf{P}}_{ir}$, i.e., for the design model we want to design a digital controller K_i to achieve $\mathbf{E}_\infty[z_j^2] \leqslant \kappa_j$ for $j = 1, 2, \ldots, n$ by using the GOVC algorithm. Store the weight Q.

Step 3: *Performance study*: Evaluate the controller K_i with the evaluation model by white noise excitation and compute the output variances. If the closed-loop system is unstable, the design specification κ_i's in step 2 are too tight and must be relaxed. Check whether $\mathbf{E}_\infty[z_i^2] \leqslant \bar{Z}_i$ for $i = 1, 2, \ldots, n$. If this is true, go to step 5; Otherwise, go to step 4 to update the design model.

Step 4: *Weighted closed-loop model*: The state-space description for the closed-loop system transfer matrix $T_i = [T_{ga} \;\; T_{s_1} \;\; T_{s_2}]$ can be obtained by using the algorithm presented in Reference 3, which uses the weight Q obtained in step 2. No model reduction is needed at this stage, i.e., high-order model of the closed-loop system is acceptable.

Step 5: Set $i = i + 1$. The plant model $\hat{\mathsf{P}}_i$ is extracted from T_i (see equation (8)). Go to step 2.

Step 6: Get the controller formula from previous iteration. **Stop**.

Remark: Notice that the performance bound $\bar{Z}_j$'s for the actual plant (not the model) can be determined based on the open-loop variances Z_j^{ol}'s (open-loop response with respect to white noise inputs if the system is stable), i.e.

$$\bar{Z}_j = \alpha_j Z_j^{ol}$$

or based on the closed-loop variances Z_j^{cl} obtained from an initial, unsatisfactory controller, i.e.

$$\bar{Z}_j = \alpha_j Z_j^{cl}$$

α_j's usually fall within the interval $[0, 1]$.

Remark: κ_j's are the performance bounds for the designed closed-loop system, i.e., the closed-loop system obtained by incorporating the controller with the model (not the actual plant). κ_j can be determined from the maximum accuracy (see Reference 12) of the model or open-loop response of the design model if the model is stable or, i.e.

$$\kappa_j = \beta_j \kappa_j^{ma}, \quad \text{or } \kappa_j = \alpha_j \kappa_j^{\text{ol}}$$

where

$$\kappa_j^{ma} = \hat{C}_{z_j} \tilde{X} \hat{C}_{z_j}^{\text{T}} + \hat{F}_{z_j} X_{\text{g}} \hat{F}_{z_j}$$
$$\kappa_j^{\text{ol}} = \hat{C}_{z_j} X \hat{C}_{z_j}^{\text{T}} + \hat{F}_{z_j} X_{\text{g}} \hat{F}_{z_j}$$

where $\tilde{X}$ satisfies equation (17) and X satisfies

$$X = \hat{A} X \hat{A}^{\text{T}} + \hat{E} X_{\text{g}} \hat{E}^{\text{T}}$$

$\hat{C}_{z_j}$ and $\hat{F}_{z_j}$ are the ith rows of the $\hat{C}_z$ and $\hat{F}_z$. $\hat{A}$, $\hat{F}_z$, $\hat{E}$, $\hat{C}_z$ are the state-space system matrices of the model $\hat{\mathsf{P}}_{ir}$ in the form of equation (9). α_j's are usually the grid points in the interval $[0, 1]$ and β_j's are usually the grid points in the interval $[1, r)$ with r being a sufficient large number, for Example 10.

6. CONTROL DESIGN FOR BENCHMARK PROBLEM

Consider using the integrated modelling and control procedure to the benchmark problem described in Section 2. The sensor measurements used here are

$$y = [x_m \;\; \ddot{x}_1 \;\; \ddot{x}_2 \;\; \ddot{x}_3 \;\; \ddot{x}_m \;\; \ddot{x}_{\text{g}}]^{\text{T}} + [w_{\text{s}}^{\text{T}} \;\; w_{\text{g}}]^{\text{T}}$$

The first model $\hat{\mathsf{P}}_{0r}$ is obtained by using q-Markov cover to the evaluation model with $q = 300$ (number of the Markov and covariance parameters to be matched), which is of order 10 (A 12th-order model can be similarly obtained, however, for the purpose of the comparison with Notre Dame's design model, a 10th-order model is generated). A GOVC controller K_0 is designed based on $\hat{\mathsf{P}}_{0r}$. This controller stabilizes the evaluation model and the achieved performance indices $J_1 \sim J_{10}$ are computed, which are much larger than those values of the Notre Dame design.[1] This means that for control purposes the model $\hat{\mathsf{P}}_{0r}$ is worse than the Notre Dame design model. We continue the procedure and the second model $\hat{\mathsf{P}}_{1r}$ of order 10 is generated from the closed-loop system of K_0 and $\hat{\mathsf{P}}_{0r}$. A GOVC controller K_1 is designed for $\hat{\mathsf{P}}_{1r}$. K_1 stabilizes the evaluation model and the achieved performance indices $J_1 \sim J_{10}$ are listed in Table I. This controller uses very large control energy to achieve interstory drift and floor acceleration performances (compare to Notre Dame design). In the third iteration, a model $\hat{\mathsf{P}}_{2r}$ of order 10 is obtained from the closed-loop system of K_1 and $\hat{\mathsf{P}}_{1r}$. A representative comparison of the transfer function from the actuator command to the 1st floor absolute acceleration for $\hat{\mathsf{P}}_{ir}$ ($i = 0, 1, 2$), the Notre Dame design model and the evaluation model is shown in Figure 4. The model generated from the open-loop model reduction (the Notre Dame design model) matches well with evaluation model at frequencies lower than 40 Hz and has large modelling error at frequencies

Table I. Achieved performance indices

	J_1	J_2	J_3	J_4	J_5
2nd iteration	0·1587	0·2337	0·9871	0·9872	0·9890
3rd iteration	0·2762	0·4205	0·5161	0·5200	0·5001
	J_6	J_7	J_8	J_9	J_{10}
2nd iteration	0·3577	0·5496	2·5489	2·5927	3·5903
3rd iteration	0·4369	0·6908	0·7197	0·9257	1·0589

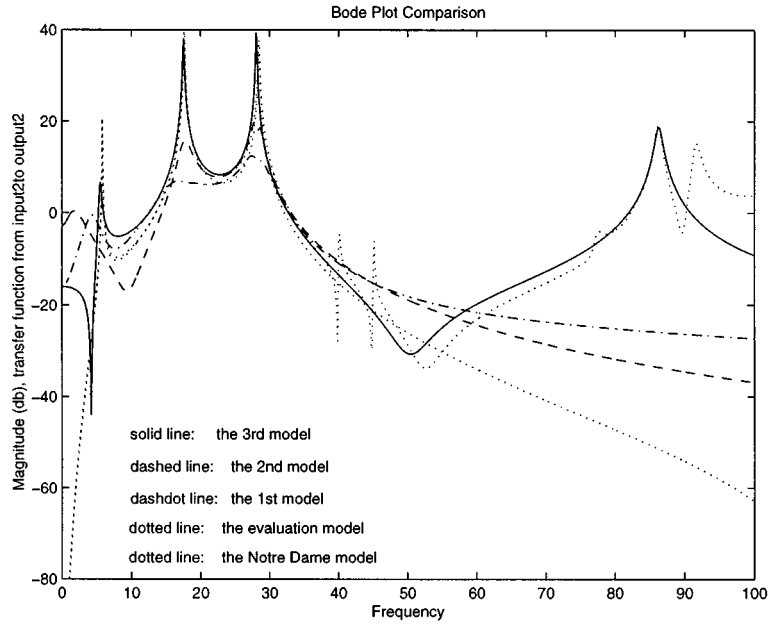

Figure 4. Bode magnitude comparison for the transfer functions of the 28th-order evaluation model (dotted line), Notre Dame 10th-order design model (dotted line), and the model generated at the 1st (dashdot line), 2nd (dotted line) and 3rd iterations (solid line). Actuator command to the 1st floor absolute acceleration

beyond 40 Hz. The model $\hat{\mathsf{P}}_{2r}$ obtained through the closed-loop modelling matches well with the evaluation model for frequencies ranged from 5 to 90 Hz, and has large modelling error for frequencies below 5 Hz. The model $\hat{\mathsf{P}}_{0r}$ and $\hat{\mathsf{P}}_{1r}$ have very large modelling errors in comparison with $\hat{\mathsf{P}}_{2r}$, however the modelling error decreases as the iteration goes. This implies that the closed-loop modelling can gradually improve the model used for the control design. Two GOVC controllers are designed from the model $\hat{\mathsf{P}}_{2r}$. One corresponds to higher control energy and the other lower controller energy. The controller with higher control energy does not meet the constraint on the loop gain (see Figure 5), and the other one does. So we take this controller as K_2. The achieved performance indices for this controller K_2, $J_1 \sim J_{10}$, are computed and are listed in Table I. (The RMS values are computed with the nominal Kanai–Tajimi parameters, $\omega_g = 37{\cdot}3$ rads/s and $\zeta_g = 0{\cdot}3$, using a simulation of 300 s duration; no maximization over (ω_g, ζ_g) was done.) For the first five criteria, the RMS values of the constraint variables are

$$\mathbf{E}_\infty[x_m^2] = 0{\cdot}6761 \text{ cm}^2, \quad \mathbf{E}_\infty[\ddot{x}_m^2] = 0{\cdot}8952 \text{ g}^2, \quad \mathbf{E}_\infty[u^2] = 0{\cdot}1585 \text{ V}^2$$

Those satisfy the hard constraints in equation (3). For evaluation criteria six through ten, the peak values of the constraint variables are

$$\max_k |x_{m_k}| = 2{\cdot}1306 \text{ cm}, \quad \max_k |\ddot{x}_{m_k}| = 4{\cdot}8307 \text{ g}, \quad \max_k |u_k| = 0{\cdot}5957 \text{ V}$$

which satisfy the hard constraints in equation (4). The loop gain transfer function is shown in Figure 5.

The time responses of the control signals, the 3rd floor absolute accelerations and the interstory drifts between the 1st and the 2nd floors for both the open- and the closed-loop system are shown in Figure 6 for El Centro earthquake excitation, and in Figure 7 for Hachinohe earthquake excitation.

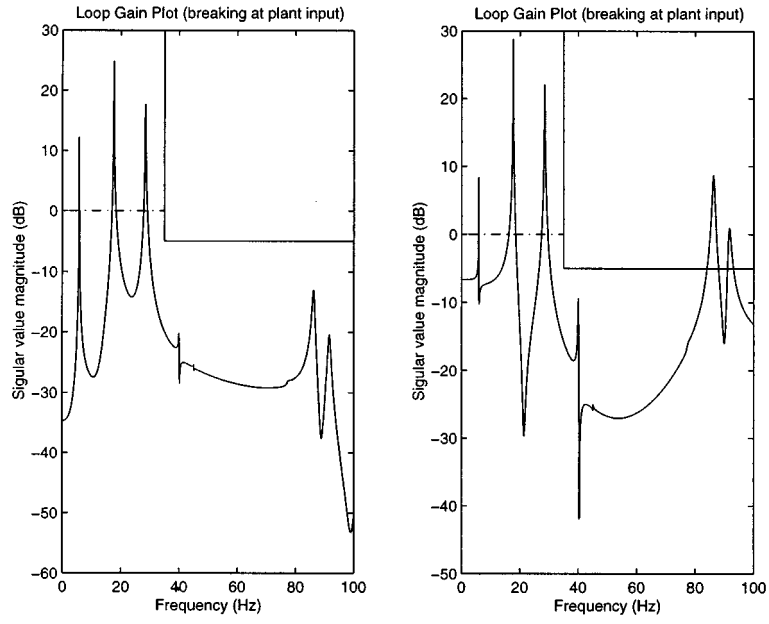

Figure 5. Loop gain transfer function for two controllers deduced for the model obtained at the 3rd iteration. The left plot shows that the lower energy controller satisfies the loop gain constraint while the right plot shows that the higher energy controller does not satisfy the loop gain constraint

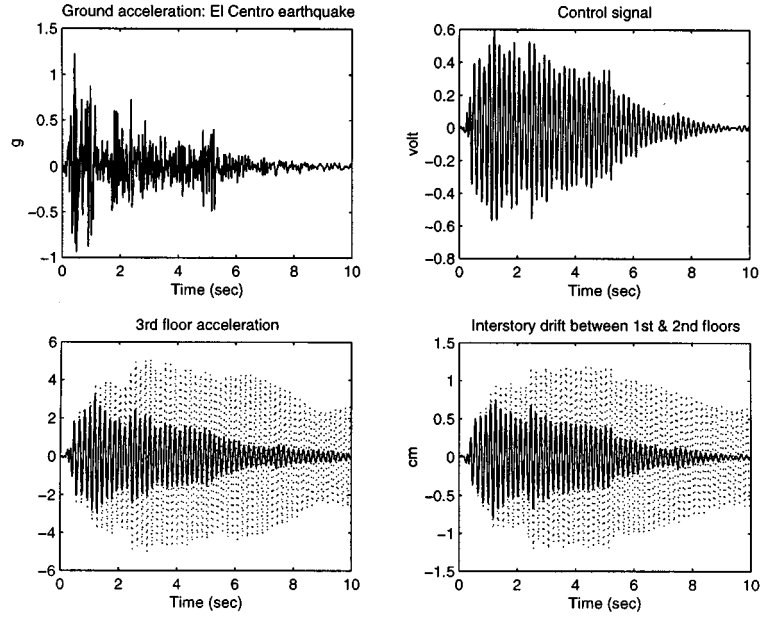

Figure 6. For the El Centro earthquake excitation, the corresponding control signal, the 3rd floor acceleration, and the interstory drift between the 1st and the 2nd floors. The dotted line indicates the open-loop responses

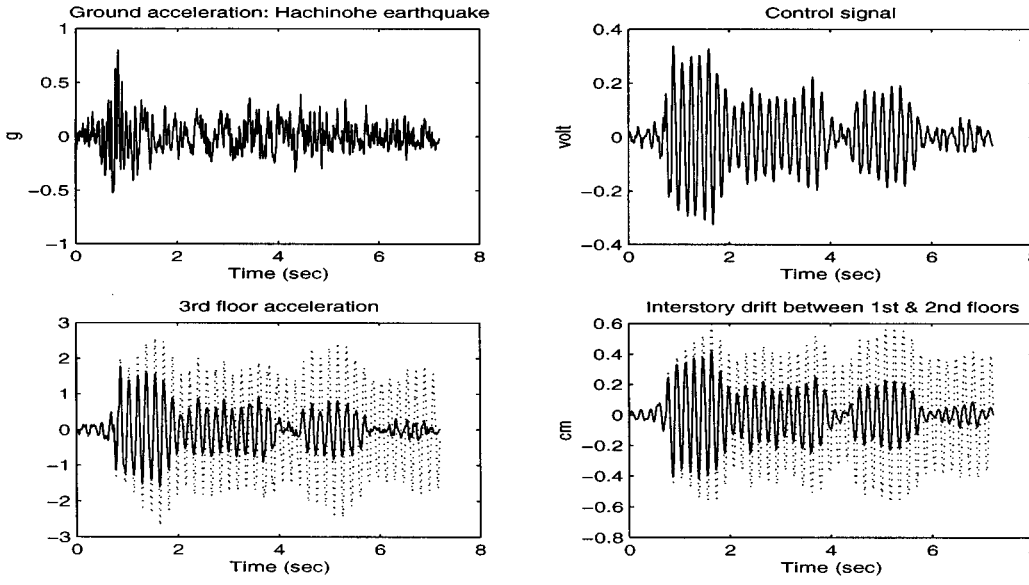

Figure 7. For the Hachinohe earthquake excitation, the corresponding control signal, the 3rd floor acceleration, and the interstory drift between the 1st and the 2nd floors. The dotted line indicates the open-loop responses

7. CONCLUSION

The iterative approach between closed-loop modelling and covariance control here can improve the model of low complexity in which many feedback related features can be preserved. Hence, a low-order controller with high performance can be achieved by our approach. In addition, the closed-loop identification is of importance in determining the dynamic behaviours of a structure where the measured data is in the closed-loop sense, hence it could be used in safety monitoring.

REFERENCES

1. B. F. Spencer Jr, S. J. Dyke and H. S. Deoskar, 'Benchmark problems in structural control. Part I — Active mass driver system', *Earthquake Engng Struct. Dyn.* **27**, 1127–1139 (1998).
2. R. E. Skelton, 'Model error concept in control design', *Int. J. Control* **49**, 1725–1753 (1989).
3. R. E. Skelton and J. Lu, 'Weighted closed-loop identification and control of civil structures', in *SPIE Proc.*, Vol. 2721, *Industrial and Commercial Applications of Smart Structures Technologies*, C. Robert Corwe (ed.), 1996, pp. 106–117.
4. S. J. Dyke, B. F. Spencer, P. Quast and M. K. Sain, 'The role of control-structure interaction in protective system design', *J. Engng. Mech.* **121**, 332–328 (1995).
5. A. M. King, U. B. Desai and R. E. Skelton, 'A generalized approach to covariance equivalent realizations for discrete systems', *Automatica* **24**, 507–515 (1988).
6. R. E. Skelton, *Dynamic Systems Control, Linear System Analysis and Synthesis*, Wiley, New York, 1988.
7. S. J. Dyke, B. F. Spencer, A. E. Belknap, K. J. Ferrell, P. Quast and M. K. Sain, 'Absolute acceleration feedback control strategies for active mass drive', *Proc. 1st World Congr. on Structural Control*, Vol. 2, 1994, pp 51–60.
8. R. E. Skelton and G. Shi, 'A weighted q-Markov cover and iterative identification and control', *Signal Process.* **52**, 217–234 (1996).
9. R. E. Skelton and J. Lu, 'Iterative identification and control design using finite-signal-to-noise models', Special issue: *Model Validation for Control Design*, *Mathematical Modelling of Systems*, Vol. 3, 102–135 (1997).
10. G. Zhu and R. E. Skelton, 'Mixed l_2 and l_∞ problems by weight selection in quadratic optimal control', *Int. J. Control* **53**, 1161–1176 (1991).
11. S. Boyd, L. E. Ghaoui, E. Feron and V. Balakrishnan, *Linear Matrix Inequality in System and Control Theory*. SIAM, Philadelphia, PA, 1995.
12. R. E. Skelton, *Dynamic Systems Control*: *Linear System Analysis and Synthesis*, Wiley, New York, 1988.

